doi:10.1006/jmbi.2001.5016 available online at http://www.idealibrary.com on IDEAL® J. Mol. Biol. (2001) 312, 1059–1071

JMB

Zooming in on the Hydrophobic Ridge of H-2D^b: Implications for the Conformational Variability of Bound Peptides

Carlo Ciatto[1], Alain C. Tissot[2], Markus Tschopp[1], Guido Capitani[1] Frédéric Pecorari[3], Andreas Plückthun[1] and Markus G. Grütter[1]*

[1]*Biochemisches Insitut, der Universität Zürich Winterthurerstrasse 190 CH-8057, Zürich Switzerland*

[2]*Cytos Biotechnology AG Wagistrasse 21, CH-8952 Zürich-Schlieren, Switzerland*

[3]*Institut de Biochimie, UMR 8619 Laboratoire de Modelisation et d'Ingenierie des Proteines, Universite Paris Sud Bat. 430, 91405, Orsay Cedex France*

**Corresponding author*

Class I major histocompatibility complex (MHC) molecules, which display intracellularly processed peptides on the cell surface for scanning by T-cell receptors (TCRs), are extraordinarily polymorphic. MHC polymorphism is believed to result from natural selection, since individuals heterozygous at the corresponding loci can cope with a larger number of pathogens. Here, we present the crystal structures of the murine MHC molecule H-2D^b in complex with the peptides gp276 and np396 from the lymphocytic choriomeningitis virus (LCMV), solved at 2.18 Å and 2.20 Å resolution, respectively. The most prominent feature of H-2D^b is a hydrophobic ridge that cuts across its antigen-binding site, which is conserved in the L^d-like family of class I MHC molecules. The comparison with previously solved crystal structures of peptide/H-2D^b complexes shows that the hydrophobic ridge focuses the conformational variability of the bound peptides in a ''hot-spot'', which could allow optimal TCR interaction and discrimination. This finding suggests a functional reason for the conservation of this structural element.

Keywords: major histocompatibility complex; T-cell receptors; antigen recognition; molecular evolution; crystal structure

Introduction

Virus-infected cells utilize the proteasome to process viral proteins; the resulting peptidic fragments are transported to the cell surface by class I major histocompatibility complex (MHC) molecules.[1] CD8$^+$ cytotoxic T-lymphocytes (CTLs) interact specifically through their surface-expressed T-cell receptors (TCRs) with the complexes between peptides and class I MHC molecules (pMHCs).[2] Activation of the CTLs triggers a series of molecular events that eventually result in the apoptosis of the infected cells.

Class I MHC molecules are dimeric proteins consisting of a heavy chain and a light chain (β_2-microglobulin). Processed peptides, deriving from both self and non-self proteins, bind in a cleft delimited on either side by an α-helix belonging to the α1 and α2 domains of the heavy chain.[3,4] The C and N termini of the bound peptides are generally buried in the binding cleft, while their middle portion can kink or arch above the cleft, exposing the central residues and making them available for interaction with the TCRs. Invariant anchor residues in the peptide sequence mediate binding to a specific class I MHC molecule allele; these are accommodated in specific pockets formed by the polymorphic residues of the heavy chain. Consequently, different class I MHC allelic products bind different sets of peptides.[3,4]

During the thymic selection of the TCR repertoire (reviewed by Goldrath & Bevan[5]), the thymocytes that carry TCRs giving rise to low-affinity interactions with MHC-bound self-peptides are positively selected, and are incorporated into the pool of mature lymphocytes circulating in the periphery. In contrast, those that recognize self-peptides with high affinity are eliminated. TCR engagement with low-affinity self-antigens is needed to ensure a pool of peripheral T-cells that

Abbreviations used: CDR, complementarity-determining region; CTL, cytotoxic T-lymphocyte; LCMV, lymphocytic choriomeningitis virus; MHC, major histocompatibility complex; pMHC, peptide/MHC complex; rms, root-mean-square; TCR, T-cell receptor.

E-mail address of the corresponding author: gruetter@bioc.unizh.ch

contains TCRs that can recognize MHCs bound to non-self peptides with high affinity. This event leads to triggering of mature CTLs. The number of slightly different peptides presented by MHC molecules, originating from pathogens but also from host proteins, is enormous. Consequently, TCRs must be able to distinguish between their cognate pMHCs and a plethora of unrelated antigens, as well as discriminate between foreign antigens among an overwhelming number of homologous self-peptides. As an additional complication, the presence of the correct anchor residues does not ensure binding to the corresponding class I MHC molecule.[6] Ultimately, the appropriate response must be delivered.

Class I MHC molecules are characterized by an unusual degree of polymorphism;[7] a large number of different alleles are represented in a population at significant frequency (>1 %). It has been proposed that heterozygosis at the MHC loci will confer the ability to bind a wider array of pathogenic peptides, thus increasing the probability of survival.[8] Support for this hypothesis has been obtained by DNA sequence analysis.[9] In brief, in the MHC exons coding for the antigen-binding region, non-synonymous nucleotide substitutions outweigh synonymous ones. In the remaining exons, the opposite phenomenon is observed. This pattern suggests that MHC polymorphism is indeed guided by natural selection. The three-dimensional structures of MHC molecules can offer an additional level of rationalization of the factors that direct MHC evolution.

The lymphocytic choriomeningitis virus (LCMV) is a non-cytopathic arenavirus pathogenic for mice. During the course of an LCMV infection, mice of the H-2^b haplotype generate a CTL response directed mainly towards three epitopes.[10] Two of them, gp33 (residues 33-41, KAVYNFATC) and gp276 (residues 276-286, SGVENPGGYCL), are derived from the viral glycoprotein; the third one, np396 (residues 396-404, FQPQNGQFI), is derived from the viral nucleoprotein. The undecameric peptide gp276 is an unusually long class I MHC-restricted epitope. All three peptides contain the anchor residue Asn in position P5, and gp276 and np396 carry a hydrophobic residue at the C terminus (P9 or P11). These two characteristics define the class I MHC molecule H-2D^b binding motif.[11]

The murine H-2D^b belongs to a group of class I MHC molecules[12] that have evolved a conserved cluster of three hydrophobic residues that form a ridge extending across the antigen-binding site.[13] We have solved the crystal structure of gp33/H-2D^b.[14] In the present study, we have determined the crystal structures of gp276/H-2D^b and np396/H-2D^b, and we have compared them to the available three-dimensional structures of peptide/H-2D^b complexes,[13–15] to elucidate the effect of the hydrophobic ridge on the conformation of the bound peptides, and to understand the possible implications for TCR recognition and class I MHC evolution.

On the basis of our structural findings, we propose that evolution has led towards conservation of this structural feature, rather than towards diversification, because the hydrophobic ridge allows optimal TCR interaction.

Results

Overall crystal structures of the LCMV peptide/H-2D^b complexes

The overall conformation of the MHC complex domains is very similar in all three structures. When compared to the gp33/H-2D^b structure,[14] the C$^\alpha$ positions of the $\alpha1/\alpha2$ peptide-binding superdomains of gp276/H-2D^b and np396/H-2D^b show root-mean-square (rms) deviation values of 0.71 Å and 0.80 Å, respectively. The comparisons of the other individual domains ($\alpha3$ and β_2-microglobulin) give rms deviations in the same range. We observed differences in the relative orientation of the single domains; however, this has been observed in analogous cases.[3] Such variations can be ascribed to the flexible connection between $\alpha1/\alpha2$ and $\alpha3$, and to differences in crystal packing.

Continuous and unambiguous electron density clearly defines the bound peptides (Figure 1). A network of hydrogen bonds connects almost all the main-chain nitrogen and carbonyl oxygen atoms to H-2D^b atoms, and keeps the peptidic backbones in an extended conformation (Figure 2(a)). Most of these hydrogen bonds are conserved across the three LCMV peptide/H-2D^b complexes (Table 1). In the previously determined structures of the complexes of H-2D^b with the influenza virus peptide np366 (residues 366-374, ASNENMETM),[13] and with the Sendai virus peptide np324 (residues 324-332, FAPGNYPAL),[15] the hydrogen bonding pattern is also the same (Table 1). The role of conserved hydrogen bonds in the binding of peptides of different sequence to the same class I MHC molecule has been discussed extensively.[3,4] As observed previously for analogous systems, the extensive network of hydrogen bonds between the protein's side-chains and the peptides' invariable main-chain atoms allows for high-affinity yet sequence-independent binding.

Gp33/H-2D^b

In the gp33/H-2D^b structure[14] there are four complexes per aymmetric unit. When considering only the bound peptide, the only remarkable difference among the non-crystallographic symmetry-related molecules is Tyr^{P4}, which exhibits two alternative conformations. In two of the molecules, the presence of crystal contacts forces the Tyr^{P4} side-chain to rotate by almost 180° around its χ_1 dihedral angle, when compared to the conformation in the other two.[14] This fact, together with the high *B*-factor value shown by Tyr^{P4} in the latter molecules, indicates a high intrinsic mobility

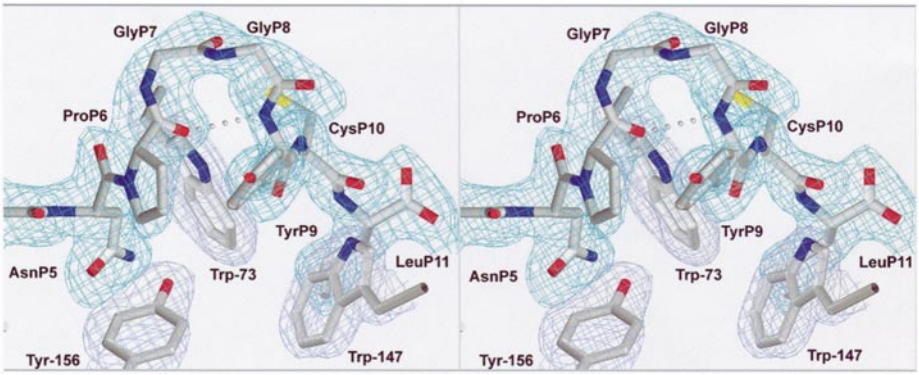

Figure 1. Zoomed view of the H-2D^b-bound gp276 peptide structure and electron density. The gp276 type I β-turn is shown (cyan density), together with the H-2D^b residues forming the hydrophobic ridge (blue density). The internal hydrogen bond is shown as grey spheres. The $2F_o - F_c$ electron density map is contoured at the 1.0 σ level. The Figure was made in SETOR.[16]

of this residue. We consider the second two molecules as representative of biological reality because there is no crystal contact in the neighborhood of the peptide. Residues Lys^{P1}, Tyr^{P4}, Phe^{P6} and Thr^{P8} each contribute more than 10 % of the solvent-accessible surface of the peptide[14] (305 Å^2 , calculated with AREAIMOL[18] using a 1.4 Å radius probe).

Np396/H-2D^b

As in other peptide/H-2D^b structures,[13–15] a hydrophobic ridge cuts through the H-2D^b binding cleft and forces the peptidic backbone to arch between Asn^{P5} and the carboxy-terminal residue Ile^{P9}, which are anchored into the D and F pockets[19] in the floor of the cleft. Residues Phe^{P1}, Phe^{P4}, Gln^{P7} and Phe^{P8} contribute 85 % of the np396 solvent accessible surface (343 Å^2).

Gp276/H-2D^b

To date, structural information on class I MHC-bound peptides of unusual length is limited to the 13 residue MTF-E peptide, complexed to the rat RT1-A^a;[20] the undecameric LCMV-derived gp276 peptide, in complex with H-2D^b, represents the second-longest peptide whose structure has been determined. The sequence of gp276 reveals the presence of two potential anchor residues at the C terminus. Most H-2D^b-restricted epitopes end with a bulky hydrophobic residue[11], which makes Leu^{P11} the most likely candidate. Conversely, the gp33/H-2D^b structure[14] indicates that also Cys^{P10} could be accomodated in the F pocket. If that were true, the C-terminal residue would extend out from the binding site; this binding mode has been observed just once so far in the case of the human HLA-A2.1 molecule in complex with a decameric peptide.[21] However, the crystal structure of gp276/H-2D^b shows that Leu^{P11} is located in the F pocket and is indeed the C-terminal anchor residue. The additional length of the undecameric gp276 peptide, which comprises five residues between the two anchors P5 and P11, is accommodated by further bulging of the peptidic chain upwards (Figure 1), away from the floor of the binding site and into the solvent, and towards the α1 α-helix (Figure 2(a)). The resulting conformation corresponds to a hydrogen-bonded type I β-turn,[22] spanning Pro^{P6} to Tyr^{P9} (Figure 1). In the MTF-E/RT1-A^a complex,[20] the longer 13 residue peptide assumed two alternative, highly solvent-exposed conformations, containing one or two (I, I + 2) double turns.[23] In gp276, Glu^{P4}, Gly^{P7}, Gly^{P8}, and Tyr^{P9} are the most solvent-accessible residues (together contibuting over 85 % of the total 347 Å^2). Interestingly, the introduction of two extra residues does not increase the gp276 total solvent accessible surface significantly, when compared to np396 (347 Å^2 *versus* 343 Å^2); and the increase is less than 15 % in comparison with gp33 (347 Å^2 *versus* 305 Å^2). Alternatively, when considering only the residues between the anchors, the solvent-accessible surface increases dramatically (242 Å^2 *versus* 172 Å^2 and 135 Å^2 , respectively). Gly^{P7} and Gly^{P8}, the β-turn central residues, are 95 % and 100 % solvent-exposed, and are the only gp276 resi-

Table 1. Conserved hydrogen bonds

Peptide position	H-bonds[a]
P1	N→OH Tyr171
	O→OH Tyr159
P2	N→O$^{\varepsilon 1}$ Glu63
	O→N$^{\zeta}$ Lys66
P4	O→N$^{\varepsilon 2}$ His155
P5	N→O$^{\varepsilon 1}$ Gln70
PΩ-1[b]	O→N$^{\varepsilon 1}$ Trp147
PΩ[c]	OT1→O$^{\gamma 1}$ Thr143
	OT1→OH Tyr84
	OT2→N$^{\delta 2}$ Asn80

[a] As identified by HBPLUS[17] using default parameters.
[b] PΩ-1 corresponds to residue P8 for the nonameric peptides, and to P10 for the undecameric gp276 peptide.
[c] PΩ corresponds to residue P9 for the nonameric peptides, and to P11 for the undecameric gp276 peptide.

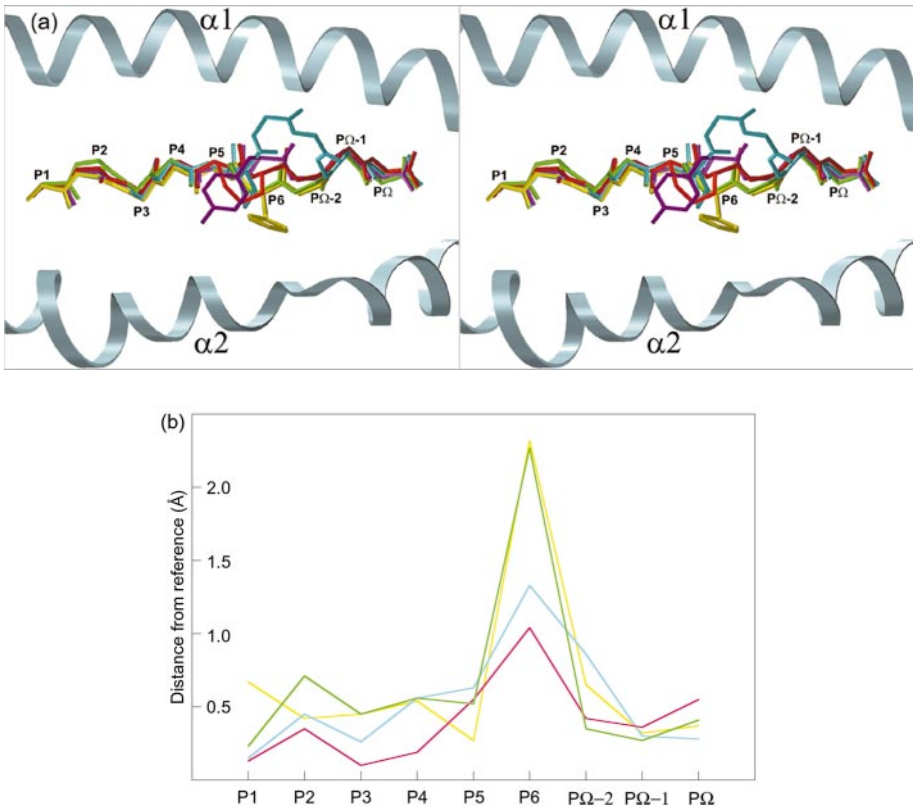

Figure 2. Structural analysis of the H-2D^b-bound peptides. The superposition is based on the C$^\alpha$ position of the α1 and α2 α-helices delimiting the binding site. (a) Top view of the binding site, showing the LCMV peptides gp33 (yellow), gp276 (cyan), and np396 (green), together with the influenza virus peptide np366 (red), and the Sendai virus peptide np324 (purple). Only the P6 side-chains are shown. PΩ represents the C-terminal residue. The two α-helices shown here belong to the reference np324/H-2D^b structure, and the remainder of the complex is omitted for clarity. The Figure was generated with SETOR.[16] (b) Graph showing the distances of the C$^\alpha$ positions from the reference peptide (np324); the color code is the same as in (a).

dues that are not involved in any hydrogen bonds. Downstream of this sequence, the main chain resumes a ''standard'' conformation: the C$^\alpha$ positions of residues P9-P11 of gp276 are almost superimposable with those of residues P7-P9 of the nonameric peptides (Figure 2(a)), and their main-chain atoms are held in position by homologous hydrogen bonds (Table 1), with the only noticeable exception of the P9/P7 pair. Therefore, in order to compare the peptides, the last three C-terminal residues can be denominated PΩ, PΩ-1, PΩ-2 (Figure 2(a)), starting from the residue that is accomodated in the F-pocket and moving backwards towards the N terminus (nomenclature as in reviews by Madden[3] and Bakalia & Collins[4]).

Comparison between the H-2D^b-bound peptides

Peptides in complex with class I MHC molecules have been compared superimposing the entire α1/α2 domains.[15,24] We have taken a somewhat different approach to perform a structural comparison between the various pMHCs. Digested protein fragments are displayed on the cell surface by MHC molecules in order to be scanned and recognized by TCRs. This interaction must be taken into account in the evaluation of the conformational differences in displayed peptides. In our comparison of the H-2D^b-bound peptides, we have tried to analyze such differences in this structural framework, by superimposing only those portions of the MHC molecules that are known to interact with the TCRs, based on biochemical[25–27] and structural[28–33] studies, namely, the α1 and α2 α-helices flanking the peptide binding groove (Figure 2(a)).

We have used the coordinates of the complexes of H-2D^b and the three LCMV-derived peptides, gp33[14] (PDB code 1fg2), gp276 and np369 (this study, PDB code 1jpf and 1jpg, respectively), as well as those with the influenza virus peptide np366[13] (PDB code 1hoc), and the Sendai virus peptide np324[15] (PDB code 1ce6). The structural superpositions and the rms deviations were calculated using Lsqman.[34] We first identified np324/H-2D^b as a reference structure, since it yields the lowest average rms deviation in the pairwise superposition of the C$^\alpha$ coordinates of the α1 and α2 helices from the different complexes. Then, we determined the rms deviations between the C$^\alpha$ positions of the peptides after aligment of the above-mentioned helices. Given the equivalence between gp276 P9-

P11 and P7-P9 of the other peptides (Figure 2(a)), we compared the full length of the reference nonameric np324 with the first six and the last three residues of the undecameric peptide; namely, the P1-P6 and the (PΩ-2)-PΩ intervals. Overall, the five peptides are highly superimposable and overlap extensively (Figure 2(a)), showing rms deviations ranging between 0.49 Å (np366) and 0.90 Å (gp33), and C^{α} displacements within 1.0 Å from the reference (Figure 2(b)). The only noticeable exception is the P6 position, which deviates between 1.0 Å (np366) to 2.3 Å (gp33) from the reference (Figure 2(b)).

The ridge formed by the three aromatic residues, Trp73 from the α1-helix and Trp147 and Tyr156 from the α2-helix, is a distinctive feature of H-2D^b.[13] The two tryptophan residues reach out from either side of the cleft, and expose their $N^{\varepsilon 1}$ atoms to the solvent. The tyrosine residue lies on the floor of the cleft, pointing its hydroxyl group towards the tryptophan residues in the center of the cleft. In combination with the highly conserved[3] hydrogen bond between Trp147 and the PΩ-1 main-chain carbonyl oxygen atom, the presence of two other potential hydrogen-bond partners offers alternative binding modes to the peptides. The two LCMV peptides gp276 and np396, as already observed for gp33,[14] fully exploit this hydrogen-bonding potential (Figure 3(a)). The main-chain carbonyl oxygen atoms of the peptide residues P6 from all three LCMV-derived antigens bind to Trp73 $N^{\varepsilon 1}$, the PΩ-2 main-chain carbonyl oxygen atoms bind to the Tyr156 hydroxyl group *via* a conserved water molecule, and PΩ-1 binds to Trp147 $N^{\varepsilon 1}$ (Figure 3(a)). This hydrogen bonding network is different from that observed (Figure 3(b)) in the previously determined structures with np366 from influenza virus,[13] and np324 from Sendai virus.[15] Despite having the same architecture of the ridge, the main-chain carbonyl oxygen atom of P6 is free, and Trp73 $N^{\varepsilon 1}$ hydrogen bonds PΩ-2; the hydrogen bond between Trp147 $N^{\varepsilon 1}$ and PΩ-1 is conserved also in this case (Figure 3(b)).

In previous crystallographic analyses of the H-2D^b binding cleft and of another class I MHC molecule, H-2L^d,[35] which possesses the same triad of aromatic residues, the hydrophobic nature of the ridge has been emphasized. In contrast, the comparison among the available H-2D^b complexes shows that its polar, hydrophilic characteristics are important determinants of the conformation of the bound peptides.

The surface hydrophobicity and hydrophilicity of a protein can be calculated and visualized using the program HydroMap.[36] The resulting hydrophobicity maps provide an intuitive, but nonetheless rigorous aid for the analysis of the interactions between proteins and ligands. Figure 4 shows the prominently hydrophilic nature of the solvent-exposed portion of the ridge. On the other hand, this feature alone cannot account for the different conformation of the five peptides bound to H-2D^b. On the α2-helix side of the ridge there is the E pocket,[19] a shallow, hydrophobic patch delimited by Ser150, Ala152 and His155 on the sides, and closed on the bottom by Trp147 and Tyr156. In the

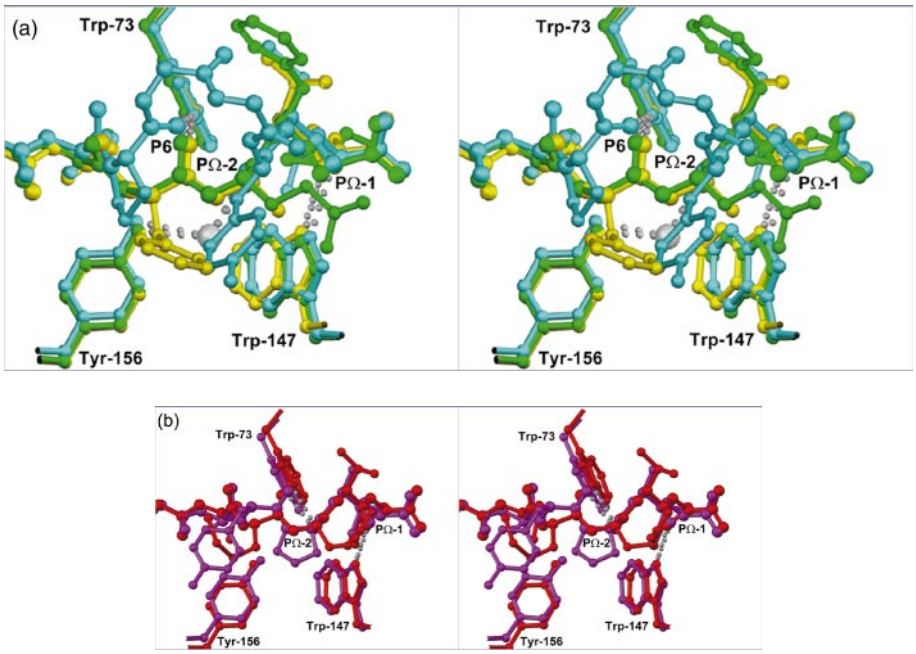

Figure 3. Alternative hydrogen-bonding patterns in the hydrophobic ridge region. The H-2D^b residues forming the hydrophobic ridge are shown, together with the bound peptides. (a) Binding mode observed in the LCMV peptide complexes. The gp33 complex is depicted in yellow, the gp276 in cyan, and the np396 in green. The hydrogen bonds and the conserved water molecule are shown as grey spheres. (b) Alternative binding mode, adopted by the np366 complex (red), and the np324 complex (purple). The hydrogen bonds are shown in grey. The Figure was made in SETOR.[16]

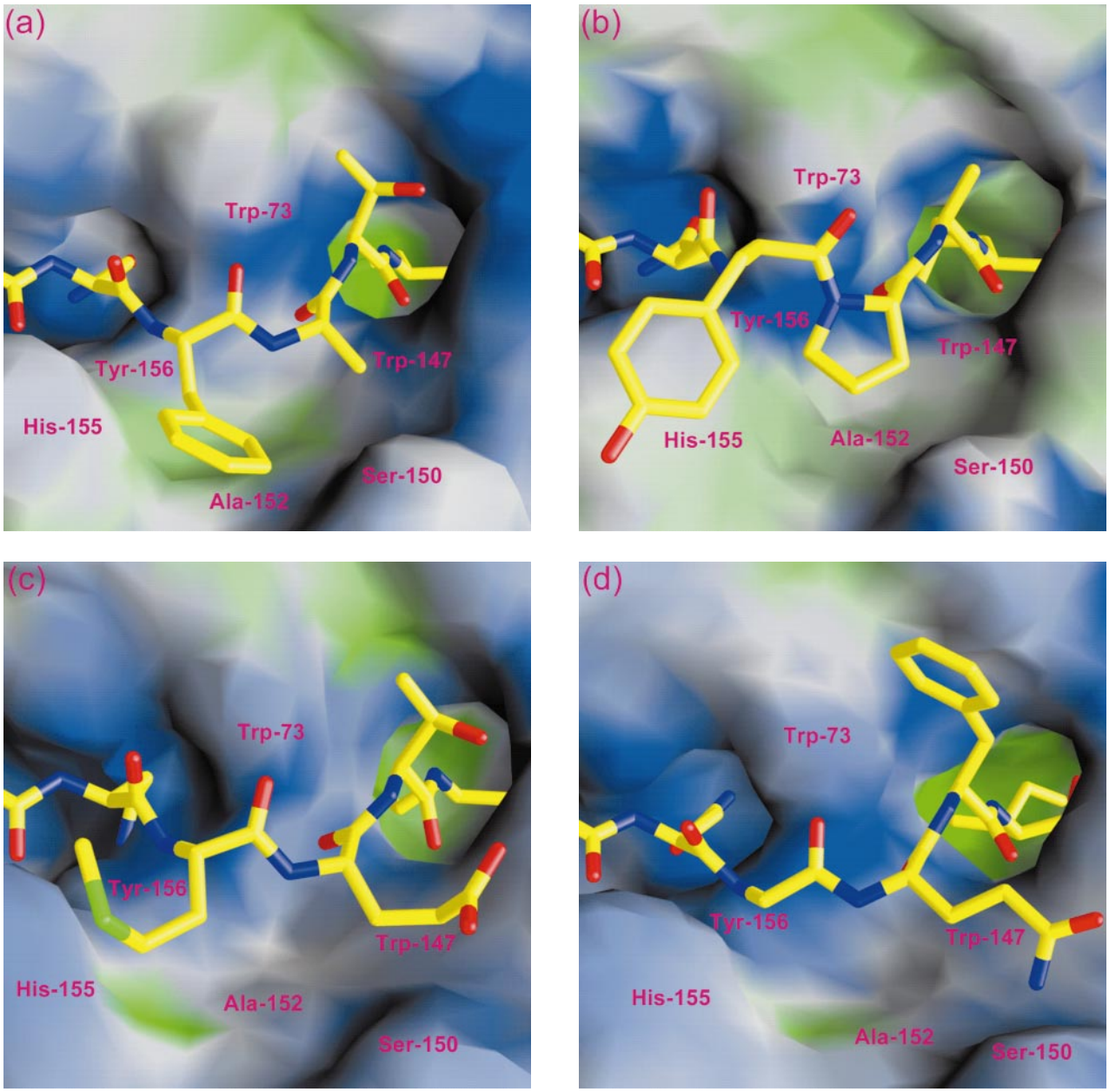

Figure 4 (*legend opposite*)

case of gp33 (Figure 4(a)), the aromatic ring of Phe^{P6} lies in the E pocket, and is in van der Waals contact with Ala152 and His155. This interaction pulls the P6 C$^{\alpha}$ towards the α2-helix. In the extreme case of np324 (Figure 4(b)), Pro^{P7} instead occupies the E pocket, close to Ala152. Tyr^{P6} stacks on top of His155, which is rotated around its χ_2 dihedral angle by almost 90° with respect to the gp33 structure. As a result, the C$^{\alpha}$ of Tyr^{P6} is now pushed towards the α1-helix. np366 (Figure 4(c)) represents an intermediate situation, with Met^{P6} interacting with His155, but leaving the E pocket vacant; consequently the C$^{\alpha}$ of Met^{P6} is positioned closer to the center of the cleft. In the np396 structure (Figure 4(d)), neither Gly^{P6} nor Gln^{P7} interact with this portion of the molecular surface of H-2D^b. The C$^{\alpha}$ of Gly^{P6} almost ovelaps with that of gp33 Phe^{P6} (Figure 2(a)). Finally, the interactions of P6 and PΩ-2 with the hydrophobic E pocket are also crucial in determining the local conformation of the longer gp276 peptide (Figure 4(e)): Pro^{P6} stacks against His155, which retains the same conformation as in the gp33/H-2D^b structure, and Tyr^{P9} comes in close proximity with Ser150 and Ala152. As a consequence, the two intervening residues, Gly^{P7} and Gly^{P8} are forced upwards and towards the α1-helix.

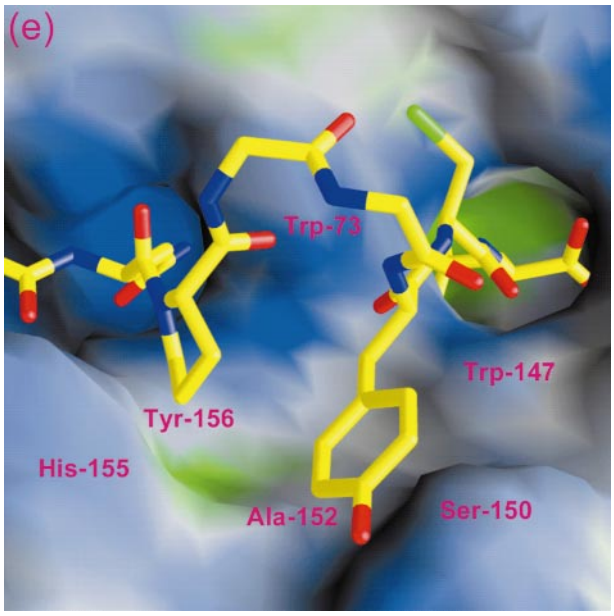

Figure 4. Surface representation of the hydrophobic ridge region in the different peptide/H-2D^b complexes. Hydrophobic areas are represented in green, and hydrophilic areas in blue. The labels indicate the positions of the H-2D^b residues that are discussed in the text. (a) gp33; (b) np324; (c) np366; (d) np396; (e) gp276. The hydrophobicity and hydrophilicity were calculated with HydroMap,[36] and rendered on the molecular surface generated in GRASP.[37]

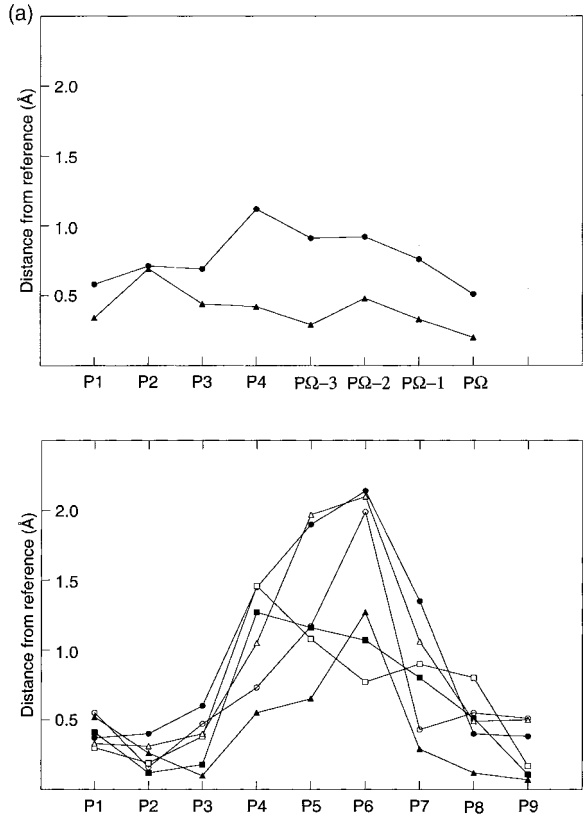

Figure 5. Variability analysis of class I MHC-bound peptides. (a) H-2K^b-restricted epitopes: C$^\alpha$ displacements from the reference peptide (VSV-8). Filled circles, SEV-9; filled triangles, OVA-8. (b) HLA-A*0201-restricted epitopes: C$^\alpha$ distances from the reference peptide (p1049). Filled circles, HIV-1 gp120; filled squares, HIV-1 RT 476-484; filled triangles, HTLV-1 Tax; open circles, calreticulin leader peptide; open squares, HIV-1 RT 309-317; open triangles, HER-2/neu GP2.

Variability among other class I MHC-bound peptides

We have structurally evaluated the variability of peptides bound to other murine as well as human class I MHC molecules, using the same procedure as for H-2D^b. In H-2K^b, the murine class I H-2K molecule belonging to the H-2^b haplotype, residues 73 and 156 are serine and tyrosine, respectively, and the floor of the peptide-binding cleft is relatively flat. The coordinates of H-2K^b in complex with two octameric peptides, VSV-8[24] (PDB code 2vaa) and OVA-8[38] (PDB code 1vac), and one nonameric peptide, SEV-9[24] (PDB code 2vab) were used. The reference structure is VSV-8/H-2K^b, and the first four and the last four residues of each peptide were used. In this case, the graph showing the C$^\alpha$ displacements does not indicate any outliers (Figure 5(a)).

Several crystal structures are available of the human class I MHC molecule HLA-A (allele A*0201) in complex with different peptides. Due to the presence of threonine 73 and leucine 156, this molecule also has a flat peptide-binding groove. Six different nonameric peptides were selected: HIV-1 gp120[39] (PDB code 1hhg), HIV-1 RT 476-484[39] (PDB code 1hhj), HTLV-1 Tax[39] (PDB code 1hhk), HIV-1 RT 309-317[40] (PDB code 1akj), HER-2/neu GP2[41] (PDB code 1qr1), and p1049[42] (PDB code 1b0 g). Also included was the decameric calreticulin leader peptide[21] (PDB code 2clr), which binds between P1 and P9 in register with the shorter ones. Figure 5(b) describes the C$^\alpha$ distances from the reference peptide (p1049/HLA-A*0201), and shows that the variability is spread across the central residues (P4 to P6).

Discussion

TCR recognition of pMHCs

Vital to the proper development and functioning of the T-cell-mediated cellular immunity is the capability of TCRs to bind and differentiate among ligands. The selection of the TCR repertoire in the thymus, and the survival and proliferation of naïve and memory T-cells in the periphery (reviewed by Goldrath & Bevan[5]), are based on the ability of TCRs to interact specifically, but with low affinity, with pMHCs.[43,44] Using an H-2D^b-restricted antigen in transgenic mice,[45] it was demonstrated how

the fate of CD8$^+$ T-cells is determined by the engagement of their TCRs with different complexes. Naïve T-cells were shown to require the presence of self-peptides bound to the restricting H-2D^b for survival, and were activated by the interaction with the correct antigen/H-2D^b complex. Memory T-cells survived independently of the nature of the MHC molecule, and proliferated in the presence of the right antigen complexed to H-2D^b.[45] A single TCR must therefore be able to discriminate between self and non-self, as well as between different antigens.

Before crystal structures of ternary TCR/peptide/MHC complexes were available, mapping of the TCR contacts on the pMHC surface[25] had delineated the topology of the TCR/peptide/MHC interaction, showing how the complementarity-determining regions (CDRs) 1 and 2 from the α and β TCR subunits interacted with the relatively conserved α-helices of the MHC molecules. The most variable TCR loops, namely the CDRα3 and β3, interact with the central part of the MHC-bound peptides. Recently, the structure determination of several ternary complexes, involving both murine[29,32,33] and human[28,30,31] MHC molecules, allowed the direct visualization of this binding mode, which assigns the discriminatory function to the α3 and β3 loops. In all cases, the TCR is oriented diagonally with respect to the pMHC surface, with the α subunit contacting the complex on the peptide N-terminal side, and the β subunit over the C-terminal one. The interaction with the peptide is always limited to a very few residues.

Of particular interest for our discussion is the role of the peptide residue P6 in the process of TCR recognition. In the case of the murine complexes (2C/dEV8/H-2K^b,[29] 2C/SIYR/H-2K^b,[32] and BM3.3/PBM1/H-2K^b[33]), which contain octameric antigens, the P6 side-chain is always involved in hydrogen bonds with the TCR. The complexes between the human molecules and the nonameric Tax peptide (A6/HLA-A2/Tax,[28] and B7/HLA-A2/Tax[30]) show only a van der Waals interaction between the TCR and the main-chain carbonyl oxygen atom of Pro^{P6}, whose side-chain is buried in the MHC antigen-binding cleft. In the complex between A6 and the HLA-A2-bound P6A mutant of the Tax peptide,[31] a low-affinity antagonist for the TCR, an enlarged cavity has been observed at the TCR-pMHC interface; this cavity is occupied only partially by a water molecule bound to the Ala^{P6} main-chain nitrogen atom. The loss in TCR affinity has been attributed to this interface defect,[46] which demonstrates the sensitivity of the pMHC recognition by TCRs also in the absence of a direct interaction.

† http://imgt.cines.fr (Initiator and coordinator: Marie-Paule Lefranc, Montpellier, France).

The hydrophobic ridge in class I MHC molecules

The analysis presented here of the crystal structures of the complexes between H-2D^b and the three LCMV peptides, and their comparison with those with the influenza virus[13] and the Sendai virus[15] peptides, shows that the hydrophobic ridge that cuts across its antigen-binding site is a distinctive structural feature of H-2D^b. Of the three residues that form the ridge, Trp73, Trp147, and Tyr156, only Trp147 is highly conserved among all MHC class I molecules (see the Kabat database[47]), while Tyr156 occupies one of the most variable positions among the H-2 gene products (Kabat database[47]). Nonetheless, it is always present, in association with Trp in position 73, in a sub-group of class I MHC alleles[12], which includes L^d, L^q, D^q, and D^b.

Interestingly, this triad of residues (Trp73, Trp147, Tyr156) is not exclusive to MHC molecules encoded by the D region of the mouse H-2 complex (H-2D and H-2L loci). The ridge is also found in the K region,[48] as well as in the Q region.[49] The latter encodes for ''non-classical'' class I MHC molecules. Conversely, no known example exists for the human HLA complex, as seen in IMGT†, the international ImMunoGeneTics database.[50] Trp147 is conserved also in the HLA complex, but neither a Trp in position 73, nor a Tyr in the highly variable position 156, have been observed to date. This finding confirms the absence of the hydrophobic ridge in the HLA molecules. Instead, a comparable ridge, formed by the protrusion of hydrophobic residues in the peptide-binding groove, is found in the rat RT1-A^a molecule.[20] In this case, three different residues, Tyr152, Trp70, and Tyr9, intersect and divide the groove at its midpoint.

An evolutionary hypothesis

The unusually high level of sequence similarity observed between the MHC class I molecule H-2L^d and a number of different MHC class I H-2D and H-2L gene products,[51] suggests the existence of an L^d-like family of molecules. Furthermore, an analysis of the primary structure conservation among the L^d-like family members demonstrates both a tight evolutionary relationship,[52] and the existence of a selective advantage in maintaining an L^d-like structure.[52] The analysis of the class I MHC antigen-binding domains,[12] using an average distance method, which groups the most similar sequences, demonstrated the presence of a cluster of evolutionarily related MHC alleles, namely L^d, L^q, D^q, and D^b. All these alleles, which are members of the L^d-like family, have both Tyr156 and Trp73, and thus possess the hydrophobic ridge.

The possibility that the maintenance of the ridge could confer an evolutionary advantage has been suggested, on the basis of sequence[52] and structural information.[13] The new structural data shown here, together with the comparative analysis of all

known H-2D^b-bound peptides, allow us to substantiate this hypothesis.

Although crystal structures of ternary complexes involving H-2D^b are unavailable, the emerging principles of pMHC recognition by TCR delineated above should be applicable also to this molecule. The protrusion of the bound peptides between P5 and PΩ, caused by the hydrophobic ridge, could correspond to an increased importance of this area, which represents the most significant fraction of the peptides' solvent-accessible surface (44 % for gp33, 50 % for np396, 62 % for np366, 70 % for gp276, and 72 % for np324). This effect is observed in the modelled ternary complex between the 2C TCR and QL9/H-2L^d.[53] The bulge in the C-terminal portion of the QL9 peptide, induced by the hydrophobic ridge, enhances the pMHC/TCR interaction by increasing the number of contacts with the QL9 C terminus. The binding-groove of the rat RT1-A^a contains a hydrophobic ridge,[20] albeit in a different position; homology modelling of the interaction between MTF-E/RT1-A^a and the 2C, A6, and B7 TCRs[20] shows close contacts involving the protruding portion of the 13 residue MTF-E peptide. In the H-2D^b complexes, the bound peptides' main chain is allowed to follow different paths between the two anchors, due to the alternative hydrogen bonding network. The localization of the H-2D^b-bound peptide variability around P6 (Figure 2(b)) might translate into optimal TCR discrimination between antigens and between self and non-self, and could justify the conservation of the hydrophobic ridge in different class I MHC alleles.

Our comparison shows that a flat binding groove, like that of the human HLA-A*0201, can allow for considerable conformational variability of the bound peptides (Figure 5(b)). The equally flat binding groove of the murine H-2K^b does not (Figure 5(a)). The solution adopted by the L^d-like molecules seems effective. It is likely that the human HLA molecules have evolved alternative strategies to permit improved TCR discrimination.

Table 2. Data collection and refinement statistics

Space group	gp33 $P2_1$	gp276 $P4_32_12$	np396 $C2$
A. *Cell parameters*			
a (Å)	92.53	56.17	91.12
b (Å)	124.77	56.17	109.95
c (Å)	99.56	277.95	57.74
α (deg.)	90	90	90
β (deg.)	103.03	90	90
γ (deg.)	90	90	122.88
Molecules per asymmetric unit	4	1	1
B. *Data collection*			
Resolution limit (Å)	2.75	2.18	2.20
Outermost shell (Å)	2.81-2.75	2.23-2.18	2.25-2.20
Unique reflections[a]	51,494 (3422)	24,648 (1569)	23,164 (1278)
Redundancy[a]	2.7 (2.3)	8.6 (6.9)	3.2 (2.4)
Completeness[a] (%)	90.8 (88.4)	99.8 (98.3)	95.6 (79.7)
Average I/σ[a]	11.7 (2.0)	22.1 (9.0)	16.7 (2.3)
R_{merge}[a,b] (%)	8.0 (38.6)	8.2 (29.3)	6.4 (34.3)
C. *Refinement*			
R-factor[c] (%)	23.6	21.1	22.8
R_{free}[d] (%)	27.6	26.2	28.8
No. water molecules	114	206	33
rmsd bonds (Å)	0.009	0.010	0.009
rmsd angles (deg.)	1.46	1.49	1.41
D. *Average B values (Å^2)*			
All protein atoms	45.9	32.8	51.9
MHC	46.2[e]	32.7	52.1
Peptide	34.8[e]	37.4	42.9
Water	36.0	35.6	39.2
E. *Ramachandran plot regions*[f]			
Most favoured regions (%)	86.4	90.6	85.2
Additional allowed regions (%)	11.1	8.8	14.2
Generously allowed regions (%)	2.0	0.6	0.6
Disallowed regions (%)	0.4	0.0	0.6

[a] Numbers in parentheses refer to the outermost resolution shell.
[b] $R_{merge} = \Sigma_{hkl}\Sigma_j|I_{j,hkl} - \langle I_{hkl}\rangle|/\Sigma_{hkl}\Sigma_j I_{j,hkl}$, where $\langle I_{hkl}\rangle$ is the average of the intensity $I_{j,hkl}$ over $j = 1,\ldots,N$ observations of symmetry-equivalent reflections hkl.
[c] R-factor $= (\Sigma_{hkl}||F_o| - |F_c||)/\Sigma_{hkl}|F_o|$, where $|F_o|$ and $|F_c|$ are the observed and calculated structure factor amplitudes, respectively.
[d] R_{free} is the same as R-factor but is calculated using 10 % of the reflections that were excluded from the refinement.
[e] This value refers to all four molecules in the asymmetric unit.
[f] Calculated with PROCHECK.[57]

Simple mathematical considerations[54] proved that T-cells must be extremely cross-reactive to ensure a complete coverage of the full universe of foreign peptides. This occurs to the extent that each single TCR could react with approximately 10^6 different pMHCs.[54] The "molecular trick" played by the L^d-like molecules could be one of many that are used to enhance the differences between MHC-bound peptides and, ultimately, might help achieve discrimination between ligands.

Materials and Methods

The peptides were synthesized and purified by Chiron Technologies (Clayton Victoria, Australia) to 95 % purity and analyzed by mass spectrometry. The plasmids encoding the H-2D^b heavy chain and β_2-microglobulin were obtained from Dr J. C. Sacchettini (Department of Biochemistry, Albert Einstein College of Medicine, New York).

Expression and purification of the peptide/H-2D^b complexes

The gp33/H-2D^b[14] was refolded in a buffer containing 0.8 M L-arginine, 200 mM Tris-HCl (pH 8.0), 2 mM EDTA, 5 mM reduced glutathione (GSH), 1 mM oxidized glutathione (GSSG). The two complexes containing the gp276 and np396 peptides were refolded in 1.0 M L-arginine, 100 mM Tris-HCl (pH 8.0), 2 mM EDTA. For the former complex, 5 mM GSH and 1 mM GSSG were added; for the latter, 0.2 mM GSH and 0.8 mM GSSG. All the complexes were purified by anion-exchange chromatography, dialyzed against 150 mM NaCl, 20 mM Tris (pH 8.0), and concentrated using Centricon centrifugal filter devices (Millipore) at 4 °C. The final solutions used for the crystallization experiments contained a 1:1 molar ratio of peptide/H-2D^b, at a total protein concentration of 5.9 mg/ml (gp33/H-2D^b), 10.6 mg/ml (gp276/H-2D^b), or 6.1 mg/ml (np396/H-2D^b). The protein concentrations were determined spectrophotometrically.[55]

Crystallization

Crystals of the three complexes were grown by the hanging drop vapor diffusion method, by mixing 2 μl of protein solution with 1 μl of reservoir solution at 4 °C. As reported,[14] in the case of gp33/H-2D^b the reservoir solution contained 0.1 M ammonium sulfate, 20 % PEG 4000, 0.1 M Hepes (pH 7.4); for gp276/H-2D^b and np396/H-2D^b it contained 0.2 M ammonium phosphate, 25 % PEG 8000, 0.1 M Tris-HCl (pH 6.4). The reservoir solutions also contained 0.02 % (w/v) sodium azide. Large single crystals were obtained in a few weeks.

Data collection and processing

Prior to data collection, the crystals were transferred into a buffer containing the reservoir solution enriched with 20 % (v/v) glycerol, and flash-frozen in a stream of liquid nitrogen at a temperature of 100 K. As described,[14] the gp33/H-2D^b data were collected to a maximum resolution of 2.75 Å, using an Enraf Nonius CuKα rotating anode X-ray source, equipped with double focusing mirrors (MacScience). The gp276/H-2D^b and np396/H-2D^b data were collected to a maximum resolution of 2.18 Å and 2.20 Å, respectively, on the Swiss-Norwegian Beam Lines, Station BM1A, at the European Synchrotron Radiation Facility (ESRF) in Grenoble, France.

The data were processed and scaled using the HKL suite of programs (Denzo and Scalepack[56]). Data statistics are presented in Table 2.

Structure solution

The structure determination was carried out using the molecular replacement method with the program AMoRe,[58] using as a search model the p1027/H-2D^b complex[42] (PDB code 1bz9), after removal of the p1027 peptide.

As described,[14] in the case of gp33/H-2D^b the structure solution indicated the presence of four complexes in the asymmetric unit. After finding two strong cross-rotation function peaks, the subsequent translation function search detected a total of four strong peaks, which corresponded to four molecules; two of them had independent orientations, while the other two were related to the first pair by simple translation. Rigid-body refinement of the four solutions from the rotational and translational search gave a correlation coefficient of 57.4 %, and an R-factor of 48.8 %.

A similar procedure was used for the structure determination of the other two peptide/H-2D^b complexes, but in this case only one complex per asymmetric unit was present. Single solutions were found and, after rigid-body refinement, the correlation coefficient and R-factor were 53.0 % and 46.6 % for gp276/H-2D^b, and 81.1 % and 39.0 % for np396/H-2D^b.

Refinement

The relative orientation of the heavy chain and β_2-microglobulin was optimized by performing independent rigid-body refinement of the two subunits with CNS.[59] Cycles of structure refinement in CNS, utilizing the maximum likelihood target, were alternated with manual rebuilding of the model in O.[60] All observed data ($|F| > 0.0\ \sigma$) at the full resolution range were used, and anisotropic B-factor correction and bulk solvent correction were applied. Torsion angle simulated annealing at 5000 K was utilized in the early stages of refinement. Model fitting in O was carried out using cross-validated σ-A-corrected[61] $2F_o - F_c$ maps. The presence of the peptides and their conformations were confirmed by using $F_o - F_c$ difference maps. Each peptide was introduced in the respective structure as a poly-alanine model, after the R_{work} and R_{free} factors had decreased below 28 % and 30 %, respectively; the appropriate side-chains were introduced in later stages.

For gp33/H-2D^b,[14] strong non-crystallographic symmetry restraints (300 kcal mol^{-1} Å^{-2}) were applied to the four molecules in the asymmetric unit. The restraints were later released for the residues that showed different orientations or backbone conformations in the four molecules, due to interactions with non-crystallographic symmetry-related mates. Grouped B-factor refinement was initially performed using one value per residue, and towards the end of refinement two B values per residue were refined, one for the backbone atoms and one for the side-chain atoms. The 4-fold non-crystallographic symmetry average maps produced with the program DM[62] were used throughout the model-building process.

The final R_{work} and R_{free} values were 23.6 % and 27.6 %, respectively (Table 2).

In the early stages of refinement of gp276/H-2D^b and np396/H-2D^b, two *B*-factors per residue were refined; at the end, individual *B*-factors were refined. The final R_{work} and R_{free} values for gp276/H-2D^b were 21.1 % and 26.2 %, respectively, and for np396/H-2D^b they were 22.8 % and 28.8 %. The crystallographic statistics are summarized in Table 2.

Calculation of hydrophobicity maps

The surface hydrophobicity was calculated with HydroMap.[36] The procedure comprises two steps: first, the binding energy of a non-polar spherical probe to the protein is evaluated, taking into account both the electrostatic and the van der Waals contibutions to the binding. Second, the binding energy is rendered on a molecular surface produced in GRASP,[37] and color-coded: green is used for the most hydrophobic regions, white for the intermediate, and blue for the hydrophilic ones.

Selection of pMHCs for comparative analysis

For the structural comparisons, the peptides were chosen according to the following criteria: (a) the presence of canonical anchor residues, as defined in the SYFPEITHI database;[63] (b) the presence of unmodified amino acids; and (c) the presence of the wild-type sequences.

Protein Data Bank accession codes

Coordinates have been deposited in the PDB with codes 1jpf and 1jpg.

Acknowledgments

We thank Mrudula Donepudi for valuable suggestions and discussions. Experimental assistance from the staff of the Swiss-Norwegian Beam Lines at ESRF (Grenoble, France) is gratefully acknowledged. This work was supported financially by the Baugartenstiftung, 8022 Zürich, Switzerland, and partially by the Swiss National Science Foundation (grant number 3100-053957.98).

References

1. York, I. A. & Rock, K. L. (1996). Antigen processing and presentation by the class I major histocompatibility complex. *Annu. Rev. Immunol.* **14**, 369-396.
2. Zinkernagel, R. M. & Doherty, P. C. (1974). Restriction of *in vitro* T cell-mediated cytotoxicity in lymphocytic choriomeningitis within a syngeneic or semiallogeneic system. *Nature,* **248**, 701-702.
3. Madden, D. R. (1995). The three-dimensional structure of peptide-MHC complexes. *Annu. Rev. Immunol.* **13**, 587-622.
4. Batalia, M. A. & Collins, E. J. (1997). Peptide binding by class I and class II MHC molecules. *Biopolymers,* **43**, 281-302.
5. Goldrath, A. W. & Bevan, M. J. (1999). Selecting and mantaining a diverse T-cell repertoire. *Nature,* **402**, 255-262.
6. Hudrisier, D., Mazarguil, H., Laval, F., Oldstone, M. B. A. & Gairin, J. E. (1996). Binding of viral antigens to major histocompatibility complex class I H-2D^b molecules is controlled by dominant negative elements at peptide non-anchor residues. *J. Biol. Chem.* **271**, 17829-17836.
7. Klein, J. (1986). *Natural History of the Major Histocompatibility Complex*, Wiley and Sons, New York.
8. Doherty, P. C. & Zinkernagel, R. M. (1975). Enhanced immunologic surveillance in mice heterozygous at the H-2 gene complex. *Nature,* **256**, 50-52.
9. Hughes, A. L. & Yaeger, M. (1998). Natural selection at major histocompatibility complex loci of vertebrates. *Annu. Rev. Genet.* **32**, 415-435.
10. Gairin, J. E., Mazarguil, H., Hudrisier, D. & Oldstone, M. B. A. (1995). Optimal lymphocytic choriomeningitis virus sequences restricted by H-2D^b major histocompatibility complex class I molecule and presented to cytotoxic T lymphocytes. *J. Virol.* **69**, 2297-2305.
11. Falk, K., Rötzschke, O., Stefanovic, S., Jung, G. & Rammensee, H.-G. (1991). Allele-specific motifs revealed by sequencing of self-peptides eluted from MHC molecules. *Nature,* **351**, 290-296.
12. Pullen, J. K., Horton, R. M., Cai, Z. & Pease, L. R. (1992). Structural diversity of the classical H-2 genes: K, D, and L^1. *J. Immunol.* **148**, 953-967.
13. Young, A. C. M., Zhang, W., Sacchettini, J. C. & Nathenson, S. G. (1994). The three-dimensional structure of H-2D^b at 2.4 Å resolution: implications for antigen-determinant selection. *Cell,* **76**, 39-50.
14. Tissot, A. C., Ciatto, C., Mittl, P. R., Grütter, M. G. & Plückthun, A. (2000). Viral escape at the molecular level explained by quantitative T-cell receptor/peptide/MHC interactions and the crystal structure of a peptide/MHC complex. *J. Mol. Biol.* **302**, 873-885.
15. Glithero, A., Tormo, J., Haurum, J. S., Arsequell, G., Valencia, G., Edwards, J. *et al.* (1999). Crystal structures of two H-2D^b/glycopeptide complexes suggest a molecular basis for CTL cross-reactivity. *Immunity,* **10**, 63-74.
16. Evans, S. V. (1993). SETOR: hardware-lighted three-dimensional solid model representations of macromolecules. *J. Mol. Graph.* **11**, 134-138.
17. McDonald, I. K. & Thornton, J. M. (1994). Satisfying hydrogen bonding potential in proteins. *J. Mol. Biol.* **238**, 777-93.
18. Collaborative Computational Project Number 4 (1994). The CCP4 suite: programs for protein crystallography. *Acta Crystallog. sect. D,* **50**, 760-763.
19. Saper, M. A., Bjorkman, P. J. & Wiley, D. C. (1991). Refined structure of the human histocompatibility antigen HLA-A2 at 2.6 Å resolution. *J. Mol. Biol.* **219**, 277-319.
20. Speir, J. A., Stevens, J., Joly, E., Butcher, G. W. & Wilson, I. A. (2001). Two different, highly exposed, bulged structures for an unusually long peptide bound to rat MHC class I RT1-A^a. *Immunity,* **14**, 81-92.
21. Collins, E. J., Garboczi, D. N. & Wiley, D. C. (1994). Three-dimensional structure of a peptide extending from one end of a class I MHC binding site. *Nature,* **371**, 626-629.
22. Venkatachalam, C. M. (1968). Stereochemical criteria for polypeptides and proteins. V. Conformation of a system of three linked peptide units. *Biopolymers,* **6**, 1425-1436.

23. Hutchinson, E. G. & Thornton, J. M. (1994). A revised set of potentials for β-turn formation in proteins. *Protein Sci.* **3**, 2207-2216.
24. Fremont, D. H., Matsumura, M., Stura, E. A., Peterson, P. A. & Wilson, I. A. (1992). Crystal structures of two viral peptides in complex with murine MHC class I H-2K^b. *Science,* **257**, 919-927.
25. Jorgensen, J. L., Esser, U., Fazekas de St Groth, B., Reay, P. A. & Davis, M. M. (1992). Mapping T-cell receptor-peptide contacts by variant peptide immunization of single-chain transgenics. *Nature,* **355**, 224-230.
26. Chang, H.-C., Smolyar, A., Spoerl, L., Witte, T., Yao, Y., Goyarts, E. C. *et al.* (1997). Topology of T cell receptor-peptide/class I MHC interaction defined by charge reversal complementation and functional analysis. *J. Mol. Biol.* **271**, 278-293.
27. Smith, K. & Lutz, C. (1997). Alloreactive T cell recognition of MHC class I molecules: the T cell receptor interacts with limited regions of the MHC class I long alpha helices. *J. Immunol.* **158**, 2805-2812.
28. Garboczi, D. N., Ghosh, P., Utz, U., Fan, Q. R., Biddison, W. E. & Wiley, D. C. (1996). Structure of the complex between human T-cell receptor, viral peptide and HLA-A2. *Nature,* **384**, 134-141.
29. Garcia, K. C., Degano, M., Pease, L. R., Huang, M., Peterson, P. A., Teyton, L. & Wilson, I. A. (1998). Structural basis of plasticity in T cell receptor recognition of a self peptide-MHC antigen. *Science,* **279**, 1166-1172.
30. Ding, Y. H., Smith, K. J., Garboczi, D. N., Utz, U., Biddison, W. E. & Wiley, D. C. (1998). Two human T cell receptors bind in a similar diagonal mode to the HLA-A2/Tax peptide complex using different TCR amino acids. *Immunity,* **8**, 403-411.
31. Ding, Y.-H., Baker, B. M., Garboczi, D. N., Biddison, W. E. & Wiley, D. C. (1999). Four A6-TCR/peptide/HLA-A2 structures that generate very different T cell signals are nearly identical. *Immunity,* **11**, 45-56.
32. Degano, M., Garcia, K. C., Apostolopoulos, V., Rudolph, M. G., Teyton, L. & Wilson, I. A. (2000). A functional hot spot for antigen recognition in a superagonist TCR/MHC complex. *Immunity,* **12**, 251-261.
33. Reiser, J.-B., Darnault, C., Guimezanes, A., Gregoire, C., Mosser, T., Schmitt-Verhulst, A.-M. *et al.* (2000). Crystal structure of a T cell receptor bound to an allogeneic MHC molecule. *Nature Immunol.* **1**, 291-297.
34. Kleywegt, G. J. & Jones, T. A. (1994). A super position. *Joint CCP4 ESF-EACBM Newsletter Protein Crystallog.* **31**, 9-14.
35. Balendiran, G. K., Solheim, J. C., Young, A. C. M., Hansen, T. H., Nathenson, S. G. & Scchettini, J. C. (1997). The three-dimensional structure of an H-2L^d-peptide complex explains the unique interaction of L^d with beta-2 microglobulin and peptide. *Proc. Natl Acad. Sci. USA,* **94**, 6880-6885.
36. Scarsi, M., Majeux, N. & Caflisch, A. (1999). Hydrophobicity at the surface of proteins. *Proteins: Struct. Funct. Genet.* **37**, 565-575.
37. Nicholls, A., Sharp, K. A. & Honig, B. (1991). Protein folding and association: insights from the interfacial and thermodynamic properties of hydrocarbons. *Proteins: Struct. Funct. Genet.* **11**, 281-296.
38. Fremont, D. H., Stura, E. A., Matsumura, M., Peterson, P. A. & Wilson, I. A. (1995). Crystal structure of an H-2K^b-ovalbumin peptide complex reveals the interplay of primary and secondary anchor positions in the major histocompatibility complex binding groove. *Proc. Natl Acad. Sci. USA,* **92**, 2479-2483.
39. Madden, D. R., Garboczi, D. N. & Wiley, D. C. (1993). The antigenic identity of peptide-MHC complexes: a comparison of the conformations of five viral peptides presented by HLA-A2. *Cell,* **75**, 693-708.
40. Gao, G. F., Tormo, J., Gerth, U. C., Wyer, J. R., McMichael, A. J., Stuart, D. I., Bell, J. I. *et al.* (1997). Crystal structure of the complex between human CD8αα and HLA-A2. *Nature,* **387**, 630-634.
41. Kuhns, J. J., Batalia, M. A., Yan, S. & Collins, E. J. (1999). Poor binding of HER-2/neu epitope (GP2) to HLA-A2.1 is due to a lack of interactions with the center of the peptide. *J. Biol. Chem.* **274**, 36422-36427.
42. Zhao, R., Loftus, D. J., Appella, E. & Collins, E. J. (1999). Structural evidence of T cell xeno-reactivity in the absence of molecular mimicry. *J. Exp. Med.* **189**, 359-370.
43. Davis, M. M., Boniface, J. J., Reich, Z., Lyons, D., Hampl, J., Arden, B. & Chien, Y-H. (1998). Ligand recognition by αβ T cell receptors. *Annu. Rev. Immunol.* **16**, 523-44.
44. Manning, T. C. & Kranz, D. M. (1999). Binding energetics of T-cell receptors: correlation with immunological consequences. *Immunol. Today,* **29**, 417-422.
45. Tanchot, C., Lemonnier, F. A., Pérarnau, B., Freitas, A. A. & Rocha, B. (1997). Differential requirements for survival and proliferation of CD8 näive or memory T cells. *Science,* **276**, 2057-2061.
46. Baker, B. M., Gagnon, S. J., Biddison, W. E. & Wiley, D. C. (2000). Conversion of a T cell antagonist into an agonist by repairing a defect in the TCR/Peptide/MHC interface: implication for TCR signaling. *Immunity,* **13**, 475-484.
47. Johnson, G. & Wu, T. T. (2000). Kabat database and its applications: 30 years after the first variability plot. *Nucl. Acids Res.* **28**, 214-218.
48. Kvist, S., Roberts, L. & Dobberstein, B. (1983). Mouse histocompatibility genes: structure and organization of a K^d gene. *EMBO J.* **2**, 245-254.
49. Watts, S., Cranmer Davis, A., Gaut, B., Wheeler, C., Hill, L. & Goodenow, R. S. (1989). Organization and structure of the Qa genes of the major histocompatibility complex of the C3H mouse: implications for the Qa function and class I evolution. *EMBO J.* **8**, 1749-1759.
50. Ruiz, M., Giudicelli, V., Ginestoux, C., Stoehr, P., Robinson, J., Bodmer, J. *et al.* (2000). IMGT, the international ImMunoGeneTics database. *Nucl. Acids Res.* **28**, 219-221.
51. Lillehoj, E. P., Myers, N. B., Lee, D. R., Hansen, T. H. & Coligan, J. E. (1985). Structural definition of a family of L^d-like molecules distributed among four of seven haplotypes compared. *J. Immunol.* **135**, 1271-1275.
52. Rubocki, R. J., Lee, D. R., Lie, W.-R., Myers, N. B. & Hansen, T. H. (1990). Molecular evidence that the H-2D and H-2L genes arose by duplication. *J. Exp. Med.* **171**, 2043-2061.
53. Speir, J. A., Garcia, K. C., Brunmark, A., Degano, M., Peterson, P. A., Teyton, L. & Wilson, I. A. (1998). Structural basis for 2C TCR allorecognition of H-2L^d peptide complexes. *Immunity,* **8**, 553-562.
54. Mason, D. (1998). A very high level of crossreactivity is an assential feature of the T-cell receptor. *Immunol. Today,* **19**, 395-404.

55. Gill, S. C. & von Hippel, P. H. (1989). Calculation of protein extinction coefficients from amino acid sequence data [published erratum appears in *Anal. Biochem*. 1990, **189**, 283]. *Anal. Biochem.* **182**, 319-326.
56. Otwinowski, Z. & Minor, W. (1997). Processing of X-ray diffraction data collected in oscillation mode. *Methods Enzymol.* **276**, 307-326.
57. Laskowski, R. A., MacArthur, M. W., Moss, D. S. & Thornton, J. M. (1993). PROCHECK: a program to check the stereochemical quality of protein structures. *J. Appl. Crystallog.* **26**, 283-291.
58. Navaza, J. (1994). AMoRe: an automated package for molecular replacement. *Acta Crystallog. sect. A,* **50**, 157-163.
59. Brünger, A. T., Adams, P. D., Clore, G. M., DeLano, W. L., Gros, P., Grosse-Kunstleve, R. W. *et al*. (1998). Crystallography & NMR system: a new software suite for macromolecular structure determination. *Acta Crystallog. sect. D,* **54**, 905-921.
60. Jones, T. A., Zou, J. Y., Cowen, S. W. & Kjeldgaard, M. (1991). Improvement methods for building protein models in electron density maps and the location of errors in these models. *Acta Crystallog. sect. A,* **47**, 110-119.
61. Read, R. (1986). Improved Fourier coefficients for maps using phases from partial structures with errors. *Acta Crystallog. sect. A,* **42**, 140-149.
62. Cowtan, K. (1994). DM: an automated procedure for phase improvement by density modification. *Joint CCP4 ESF-EACBM Newsletter Protein Crystallog.* **31**, 34-38.
63. Rammensee, H.-G., Bachman, J., Emmerich, N. P. N., Bachor, O. A. & Stefanovic, S. (1999). SYFPEITHI: database for MHC ligands and peptide motifs. *Immunogenetics,* **50**, 213-219.

Edited by I. A. Wilson

(Received 11 April 2001; received in revised form 15 August 2001; accepted 16 August 2001)